JOURNAL OF VIROLOGY, Dec. 2005, p. 15314–15322 Vol. 79, No. 24
0022-538X/05/$08.00+0 doi:10.1128/JVI.79.24.15314–15322.2005

Soluble Receptor-Mediated Targeting of Mouse Hepatitis Coronavirus to the Human Epidermal Growth Factor Receptor

T. Würdinger,[1,2]† M. H. Verheije,[1,2]† K. Broen,[1] B. J. Bosch,[1] B. J. Haijema,[1] C. A. M. de Haan,[1] V. W. van Beusechem,[2] W. R. Gerritsen,[2] and P. J. M. Rottier[1]*

Virology Division, Department of Infectious Diseases & Immunology, Utrecht University, 3584 CL Utrecht,[1] and Division of Gene Therapy, Department of Medical Oncology, VU University Medical Center, 1081 HV Amsterdam,[2] The Netherlands

Received 5 August 2005/Accepted 27 September 2005

The mouse hepatitis coronavirus (MHV) infects murine cells by binding of its spike (S) protein to murine CEACAM1a. The N-terminal part of this cellular receptor (soR) is sufficient for S binding and for subsequent induction of the conformational changes required for virus-cell membrane fusion. Here we analyzed whether these characteristics can be used to redirect MHV to human cancer cells. To this end, the soR domain was coupled to single-chain monoclonal antibody 425, which is directed against the human epidermal growth factor receptor (EGFR), resulting in a bispecific adapter protein (soR-425). The soR and soR-425 proteins, both produced with the vaccinia virus system, were able to neutralize MHV infection of murine LR7 cells. However, only soR-425 was able to target MHV to human EGFR-expressing cancer cells. Interestingly, the targeted infections induced syncytium formation. Furthermore, the soR-425-mediated infections were blocked by heptad repeat-mimicking peptides, indicating that virus entry requires the regular S protein fusion process. We conclude that the specific spike-binding property of the CEACAM1a N-terminal fragment can be exploited to direct the virus to selected cells by linking it to a moiety able to bind a receptor on those cells. This approach might be useful in the development of tumor-targeted coronaviruses.

The search for additional cancer therapies continues as many different nonconventional approaches are being explored. The use of viruses in the fight against cancer started already in the 1950s, and several oncolytic vectors are now being evaluated in clinical trials (28, 30). The mouse hepatitis coronavirus (MHV) possesses several attractive features that suggest its possible use as an oncolytic virus. These include fast replication, syncytium formation, and cell killing, as well as species specificity. However, in order to exploit its oncolytic potential, the ability to redirect the virus to human cancer cells is a prerequisite. In order to achieve tumor-specific virus entry, different targeting approaches have been explored for a variety of viruses. These include pseudotyping, modification of viral surface proteins, and the use of bispecific adapters (14, 28, 37).

MHV belongs to the family *Coronaviridae*, a family of large (approximately 30-kb), positive-strand RNA viruses. MHV displays high species specificity, determined by the interaction between the virus spike (S) protein and the virus receptor (3). The S protein is a type I glycoprotein, synthesized as a 180-kDa glycosylated precursor that is posttranslationally cleaved into two 90-kDa subunits, S1 and S2 (13). The spike N-terminal S1 subunit is responsible for binding to the MHV receptor, which results in a conformational change of the S2 subunit, mediating the fusion of the virus envelope and the cell membrane. Key events in this fusion process are the insertion of an as-yet-unidentified fusion peptide present in the S protein into the cell membrane and the coalescence of the heptad repeat regions, HR1 and HR2, into a tightly associated six-helix bundle (2, 31).

MHV infects murine cells via receptors belonging to the carcinoembryonic antigen family of glycoproteins in the immunoglobulin (Ig) superfamily, called murine CEACAMs (1, 7, 8, 38). Results from infection studies with mice have shown that mCEACAM1a is the major receptor for MHV strain A59 (18). Through analysis of recombinant forms of CEACAM1a, it was established that the N-terminal domain is responsible for virus binding (9, 36). Crystallization studies revealed that this domain resembles an Ig-like fold and identified the amino acids responsible for interaction with the S protein (33). Furthermore, it was reported that incubation of virions with anchorless soluble receptor proteins caused a marked increase in the hydrophobicity of the virions, which was associated with a conformational change in S2 and neutralization of infection of murine cells (24, 34, 40).

The aim of our studies is to investigate the possibilities of using animal coronaviruses as oncolytic vectors for human use. This requires specific targeting of the viruses to antigens (over) expressed on tumor cells. Our approach is to engineer bifunctional adapters of which, when functioning, the sequence will be incorporated genomically into the virus to create a self-targeted vector. In a previous study, we showed that the feline infectious peritonitis coronavirus (FIPV) could be redirected to human cancer cells expressing the epidermal growth factor receptor (EGFR) via a bispecific single-chain antibody capable of binding simultaneously to the FIPV spike protein and to the human EGFR. The same adapter was also able to target fMHV, an MHV derivative carrying the FIPV spike protein, to the EGFR (39). Unfortunately, subsequent attempts to genomically incorporate the adapter sequence failed; the virus

* Corresponding author. Mailing address: Virology Division, Department of Infectious Diseases & Immunology, Utrecht University, 3584 CL Utrecht, The Netherlands. Phone: 31 30 253 2485. Fax: 31 30 253 6723. E-mail: p.rottier@vet.uu.nl.

† T.W. and M.H.V. contributed equally to this work.

appeared to be unstable and rapidly lost the inserted sequence (unpublished observations). In the present study, we therefore took a fundamentally different approach by designing an adapter of a different nature. We hypothesized that the N-terminal domain of CEACAM1a (soR), when fused to a cancer cell-binding ligand, could also be used as a bridging adapter. To demonstrate this principle, the soR part was fused to single-chain monoclonal antibody (MAb) 425 directed against the EGFR and analyzed for its capacity to mediate EGFR-specific entry of MHV into human cancer cells. The results show that although the binding of the soR moiety to the S protein presumably triggers in the viral spike the conformational changes that normally initiate the membrane fusion process, these events do not inactivate the particles but allow the fusion process to ensue as soon as the virus-adapter complex has docked with the cell receptor.

MATERIALS AND METHODS

Viruses, cells, and antibodies. Stocks of MHV-EFLM (5) and fMHV (21) were produced and titrated as before; MHV-EFLM is a derivative of MHV strain A59 that contains a firefly luciferase gene between the E and M genes (5). Recombinant vaccinia virus vTF7-3 containing the bacteriophage T7 RNA polymerase gene was used as a T7 RNA polymerase source for T7 promoter-driven production of the soR adapter proteins in OST7-1 cells (10). OST7-1 (10) (obtained from B. Moss), BHK-21 (American Type Culture Collection [ATCC]), A431 (ATCC), and LR7 (21) cells were grown in Dulbecco's modified Eagle's medium (Cambrex Bio Science, Verviers, Belgium) containing 10% fetal bovine serum, 100 IU of penicillin/ml, and 100 μg of streptomycin/ml (all from Life Technologies, Ltd., Paisley, United Kingdom). Rabbit antiserum k134, raised against purified MHV, was described previously (29). Polyclonal antibody anti-N-CEACAM-Fc, directed against the mCEACAM1a N domain, was kindly provided by T. Gallagher (15). Anti-Myc antibody 9E10 (culture supernatant from hybridoma cell line 9E10 [ATCC]) was used to detect Myc-tagged adapter proteins.

Construction of soR adapters. To obtain the gene encoding the N-terminal domain of the mCEACAM1a receptor (henceforth referred to as soR), a PCR was performed on plasmid pCEP4:sMHVR-Ig (kindly provided by T. Gallagher (15) with forward primer 2296 (5′-CATGGGCCCAGCCGGCCGAGCTGGCC TCAGCACAT-3′) and reverse primer 2297 (5′-CATGGCGGCCGCGGGGTG TACATGAAATCG-3′). In addition, PCRs were performed on the same plasmid with primers 2296 and 2298 (5′-TGTCACAAGATTTGGGCTGGGGTGT ACATGAAATCG-3′), 2296 and 2299 (5′-CGGTGGGCATGTGTGAGTTTT GTCACAAGATTTG-3′), and 2296 and 2300 (5′-CATGGCGGCCGCTGGGC ACGGTGGGCATGTGT-3′) to generate a similar soR fragment with a 3′ extension encoding a hinge linker region derived from human IgG1 (15). The resulting DNA fragments, soR (429 nucleotides) and soR-h (472 nucleotides), contained a 5′ SfiI site and a 3′ NotI site (underlined in the primers) and were subsequently cloned with these restriction enzymes into the expression vector pSecTag2 (Invitrogen, Breda, The Netherlands). The resulting expression vectors, pSTsoR and pSTsoR-h, encode the N domain of mCEACAM1a in fusion with an amino-terminal Igκ signal sequence and a carboxy-terminal myc-His tag under the control of a cytomegalovirus and a T7 promoter. The hinge region in pSTsoR-h is located directly downstream of the N domain of mCEACAM1a. Single-chain MAb 425, directed against EGFR, was isolated from pSTCFS11-425 (17, 26) by NotI digestion and ligated in a V_H-V_L configuration into the NotI site downstream of the soR and soR-h sequences in pSTsoR and pSTsoR-h, creating a three-Ala linker between the soR and single-chain fragments, resulting in expression vectors pSTsoR-425 and pSTsoR-h-425. The composition of the adapter genes was confirmed by sequencing.

Production and analysis of soR constructs. For production of the soR adapter proteins, subconfluent monolayers of OST7-1 cells were inoculated at a multiplicity of infection (MOI) of 5 with vTF7-3 ($t = 0$ h) and transfected ($t = 1$ h) with pST-soR, pST-soR-h, pST-soR-425, or pST-soR-h-425 or mock transfected by using Lipofectin (Life Technologies, Ltd., Paisley, United Kingdom). The medium was refreshed at $t = 4.5$ h, harvested at $t = 20$ h, and centrifuged for 10 min at 3,000 rpm to clear it of cell debris. The supernatants containing the soR proteins were loaded onto a 20% sucrose cushion and centrifuged for 30 min at 13,000 rpm to clear them of vTF7-3 virus prior to 20-fold concentration with Vivaspin columns. The protein batches were aliquoted and stored at −20°C.

Western blot assay. The concentrated soR adapter protein preparations were analyzed by sodium dodecyl sulfate-polyacrylamide gel electrophoresis and subsequent blotting on a polyvinylidene difluoride membrane (Bio-Rad Laboratories, Hercules, CA). To block nonspecific antibody binding, the blot was incubated in blocking buffer (phosphate-buffered saline [PBS] containing 5% Protivar and 0.05% Tween 20) for 30 min at room temperature. Incubation was continued with anti-N-CEACAM-Fc antibodies diluted 1:3,000 in blocking buffer for 1 h at room temperature, followed by swine anti-rabbit peroxidase (DAKO, Glostrup, Denmark) diluted 1:3,000 in blocking buffer for 1 h at room temperature. Finally the blot was incubated with a 1:1 mixture of luminol and enhancer (Amersham Pharmacia Biotech Europe GmbH, Freiburg, Germany) and analyzed with Hyperfilms (Amersham Pharmacia Biotech Europe GmbH) according to the manufacturer's protocol.

Anti-N-CEACAM-Fc dot blot assay. The concentration of the soR proteins in our concentrated preparations was determined by dot blot analysis. Serial dilutions in a total volume of 50 μl were blotted onto a nitrocellulose membrane with a vacuum pump. A standard curve of purified N-CEACAM-Fc protein (100 nM) was prepared in parallel to estimate the concentration of the soR adapter proteins in our preparations. The immunoassay with antibodies directed against N-CEACAM-Fc was performed as described above for the Western blot assay. The density per square millimeter of each dot was measured with a densitometer (Bio-Rad Laboratories) and plotted against the corresponding dilution factor, after which the soR protein concentrations were calculated. The different preparations were brought to the same concentration with culture medium before use.

Determination of luciferase expression. At the indicated time points, the culture media were removed and the cells were lysed with the appropriate buffer provided with the firefly assay system (Promega). Intracellular luciferase expression was measured according to the manufacturer's instructions, and the relative light units were determined with a LUMAC biocounter M2500.

Anti-MHV immunostaining. Cells inoculated with MHV or fMHV in the presence or absence of adapter protein were fixed with PBS containing 3.7% paraformaldehyde, permeabilized with PBS containing 1% Triton X-100, and subsequently incubated with k134 anti-MHV serum diluted 1:300, followed by swine anti-rabbit peroxidase (DAKO, Glostrup, Denmark) diluted 1:300, both in PBS containing 5% fetal bovine serum. The cells were stained with AEC (Brunschwig, Amsterdam, The Netherlands) according to the manufacturer's protocol and analyzed by light microscopy.

Antibody blocking experiments. To determine whether soR-425 and soR-h-425 interact with the EGFR, 10^5 A431 cells per 0.32-cm^2 well were incubated with or without 100 μl hybridoma supernatant containing MAb 425 for 30 min at 4°C. Next, the cells were inoculated with 10^4 tissue culture infective doses ($TCID_{50}$) of MHV-EFLM preincubated for 1 h at 4°C with 0.5 nM soR-425 or soR-h-425 and were incubated for 1 h at 37°C. The cells were washed, and incubation was continued for 20 h, after which they were lysed and luciferase expression was measured.

Analysis of the effect of mHR2 on coronavirus infection. The effect of fusion-inhibitory peptide mHR2 on the targeted infection process was analyzed by preparing in parallel three sets of inoculation mixtures. MHV-EFLM at 10^4 $TCID_{50}$ was preincubated in duplicate with 5 nM soR-425, soR-h-425, or mock supernatant for 1 h at 4°C. To one of each set of mixtures, mHR2 peptide was added to a concentration of 20 μM. Cultures of 10^5 human A431 cells were washed with PBS and inoculated with the infection mixtures for 1 h at 37°C. The cells were then washed and incubation continued for 20 h. Finally, the cells were lysed and luciferase activity was measured.

Monitoring of productive infection. A431 cells were seeded at 5×10^5/10-cm^2 well and inoculated the next day with 2.5×10^6 $TCID_{50}$ MHV-EFLM in the presence or absence of adapter protein for 1 h. The cells were washed three times with PBS and cultured for up to 48 h. At several time points after inoculation, a small sample of the medium was harvested, centrifuged for 10 min at 3,000 rpm, and stored at −80°C until analysis. The amount of virus produced at each time point after inoculation was determined by endpoint dilution on murine LR7 cells.

Measurement of soR-425-mediated cell-cell fusion. A431 cells at 5×10^4/0.32-cm^2 well were inoculated for 2 h with 5×10^4 $TCID_{50}$ MHV-EFLM preincubated with 5 nM soR-425 for 1 h at 4°C. The cells were washed three times with PBS and incubated further in the presence or absence of 5 nM soR-425, soR-h-425, or mock control supernatant. Immunostaining was performed at 24 h after inoculation, and the number of nuclei per syncytium was determined by counting under a light microscope.

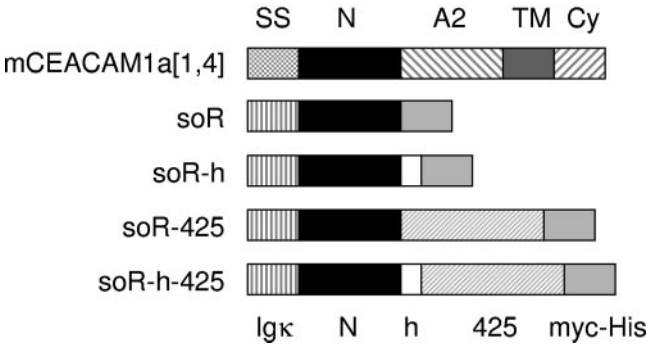

FIG. 1. Schematic diagram of the soR constructs used in this study. Native mCEACAM1a[1,4] is composed of two ectodomains (N and A2) and contains a signal sequence (SS). The N and A2 domains are linked to the transmembrane (TM) and cytoplasmic (Cy) domains. The soluble receptor constructs are depicted below mCEACAM1a[1,4], i.e., the CEACAM1a N domain (soR), the Ig hinge region (h), and single-chain MAb 425 (425). The different soR proteins contain an Igκ leader sequence for secretion and a myc-His tag for detection.

RESULTS

Construction and analysis of soR adapter proteins. In order to redirect MHV to receptors overexpressed on human cancer cells, different adapter proteins were designed that were composed of the N domain of CEACAM1a (soR) fused to anti-EGFR single-chain MAb 425 (soR-425). In addition, adapter proteins were constructed in which an IgG Fc hinge region—responsible for disulfide linkage of IgG heavy chains—was present between soR and single-chain MAb 425 (soR-h-425). Similar constructs composed of the CEACAM1a N domain only, named soR and soR-h, functioned as control proteins for the soR-425 and soR-h-425 adapters (Fig. 1). The proteins were expressed in OST7-1 cells by vTF7-3 infection and subsequent transfection with the expression constructs. Their expression was confirmed by immunostaining of the cells with anti-Myc and anti-N-CEACAM-Fc antibodies (data not shown). Next, release of the soluble receptor proteins into the culture medium was demonstrated by Western blotting (Fig. 2A, left side). The apparent molecular masses of soR, soR-h, soR-425, and soR-h-425 were slightly higher than those calculated (18.9, 20.6, 46.0, and 47.6 kDa, respectively), because of their glycosylation (data not shown). To determine whether the presence of a hinge region resulted in protein dimerization, the proteins were analyzed by sodium dodecyl sulfate-polyacrylamide gel electrophoresis under nonreducing conditions, followed by Western blotting with anti-N-CEACAM-Fc antibodies (Fig. 2A, right side). Dimerization was indeed observed for soR-h and soR-h-425, but not for soR and soR-425, which lack the

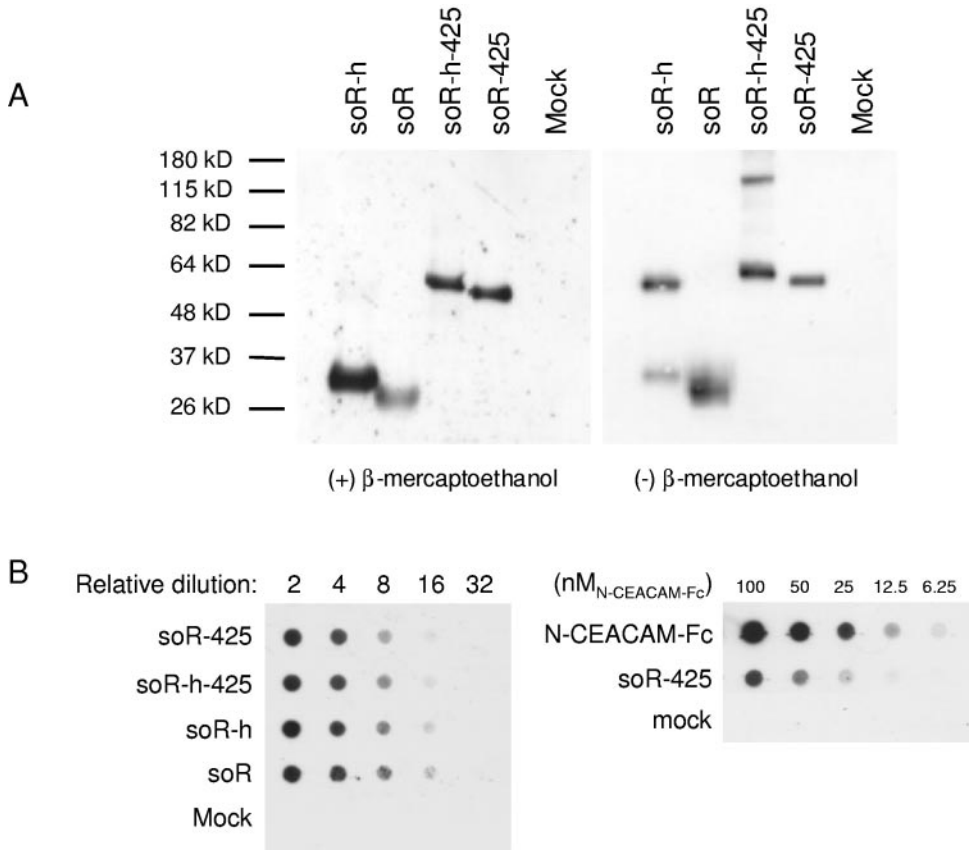

FIG. 2. Immunoblot analysis of the soR adapter proteins. (A) Western blot analysis of the soR adapter proteins in the presence (left side) and absence (right side) of β-mercaptoethanol. kD, kilodaltons. (B) Anti-N-CEACAM-Fc dot blot analysis was used to equalize the soR protein concentrations in the different batches. Twofold dilutions were made and analyzed for reactivity with anti-N-CEACAM-Fc antibody. In addition, the adapter concentration in the soR preparation was determined by an anti-N-CEACAM-Fc dot blot assay in which a standard curve of purified N-CEACAM-Fc protein (100 nM) was used to estimate the concentration of the soR adapter batches, as shown here for soR-425.

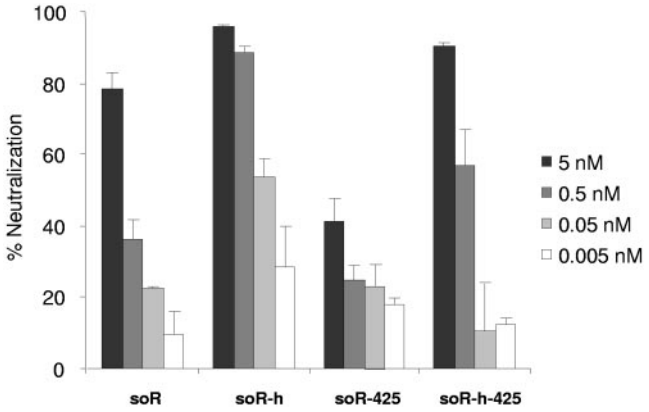

FIG. 3. Virus neutralization by the soR adapter proteins. MHV-EFLM (MOI, 0.1) was preincubated for 1 h at 4°C with various concentrations of the different soR adapter proteins and inoculated onto 10^5 murine LR7 cells, which were then incubated for 1 h. The cells were washed, incubation was continued, and after 7 h luciferase expression was measured. Shown is the percent neutralization, calculated as the decrease in luciferase expression relative to infections in the absence of adapter protein. The data represent the average of a representative experiment performed in triplicate. Error bars indicate standard deviations.

hinge region. Dimerization was, however, not complete as also monomers of the hinge-containing proteins were detected. The different soR adapter batches were titrated with the anti-N-CEACAM-Fc dot blot assay and diluted to the same concentration of anti-N-CEACAM antibody-reacting protein (Fig. 2B, left side). The concentrations of the soR adapter batches used were 25 to 50 nM, as determined by comparison to a standard of N-CEACAM-Fc protein (Fig. 2B, right side).

Soluble receptor-mediated neutralization of MHV infection on murine cells. Various forms of the CEACAM1a ectodomains can neutralize MHV by binding to the MHV spike protein (24, 34, 40). To evaluate the binding of the soR proteins to the virus, neutralization experiments were carried out. MHV-EFLM (5), a recombinant MHV-A59 strain containing a firefly luciferase reporter gene, was preincubated with various amounts of soR or its derivatives. After inoculation for 1 h, the LR7 cells were washed and incubation continued for 7 h, after which luciferase activity was measured (Fig. 3). All adapter proteins appeared to have neutralized viral infectivity, as opposed to infections carried out in the presence of mock control supernatant. Strikingly, the presence of a hinge region in the proteins resulted in increased neutralizing activity compared to the proteins lacking this region. Moreover, fusion of single-chain MAb 425 to the soR domain resulted in decreased neutralization efficiency compared to soR alone. This effect, however, was completely normalized to soR neutralization levels by the presence of the hinge region in soR-h-425.

Soluble receptor-mediated MHV infection of cells expressing human EGFR. To determine whether MHV can be redirected via the N domain of mCEACAM1a to cells lacking the MHV receptor, MHV-EFLM was preincubated with 0.5 nM soR-425 or with mock supernatant. The viruses were inoculated for 1 h onto EGFR-overexpressing human A431 cancer cells, after which the cells were washed and incubated further. At several time points after inoculation, intracellular luciferase expression was monitored to determine whether MHV infection was taking place. As shown in Fig. 4A, significant luciferase expression became measurable at 9 h after inoculation and reached a maximum at 20 h after inoculation, indicating that MHV-EFLM had successfully entered the human cancer cells in the presence of soR-425. That this infection was dependent on the activity of the adapter protein was evident from the lack of luciferase expression in its absence.

Next, the efficiencies of the targeted infections established by soR-425 and soR-h-425 were compared. To this end, MHV-EFLM was inoculated for 1 h on human A431 cells in the presence of different amounts of the soR adapter proteins. The cells were washed, and incubation was continued in normal culture medium. After 20 h, the cells were lysed and luciferase expression was measured. Figure 4B shows that the expression of luciferase was dependent on the dose of soR-425 or soR-h-425. In contrast, MHV-EFLM preincubated with soR, soR-h,

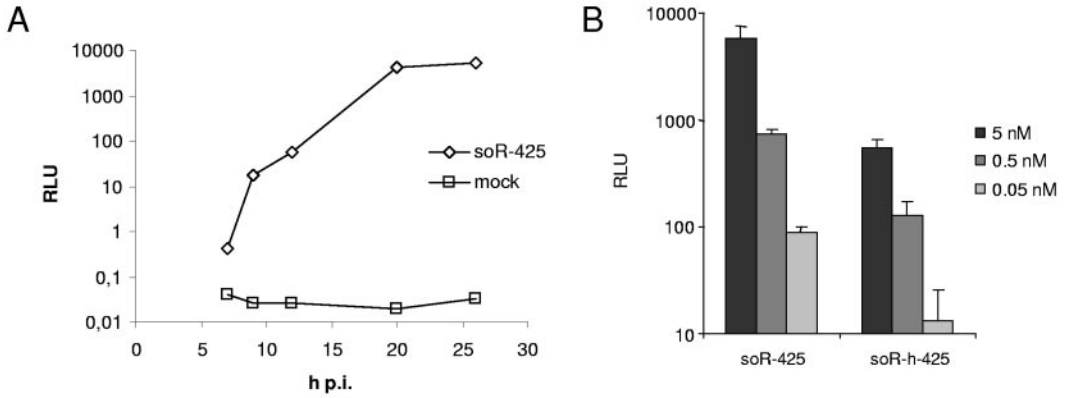

FIG. 4. Targeting of MHV-EFLM to human A431 cells. (A) To determine whether MHV-EFLM was able to infect human A431 cells, 10^4 $TCID_{50}$ of MHV-EFLM were preincubated in the presence or absence of 0.5 nM soR-425. After inoculation onto 10^5 A431 cells for 1 h at 4°C, the cells were washed and incubated further. At several time points after inoculation, intracellular luciferase expression was measured. Shown are the data from a representative experiment. (B) MHV-EFLM (10^4 $TCID_{50}$) was preincubated with the different soR adapter proteins at various concentrations and inoculated onto A431 cells, which were incubated for 1 h. At 20 h after inoculation, luciferase expression was determined. All data shown represent the average and standard deviation of an experiment performed in triplicate. RLU, relative light units; p.i., postinoculation.

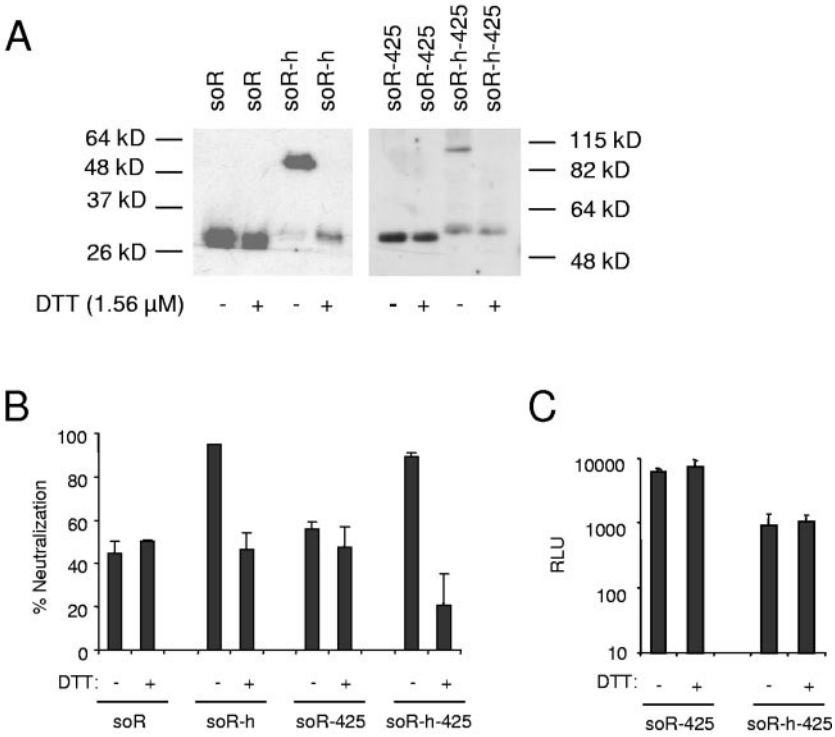

FIG. 5. Soluble receptor-mediated MHV neutralization, but not targeting, is affected by soR dimer formation. (A) Western blot analysis of the soR adapter proteins electrophoresed under nonreducing conditions after preincubation in the presence (+) or absence (−) of DTT. kD, kilodaltons. (B) MHV-EFLM (MOI, 0.1) was inoculated onto murine LR7 cells, which were incubated for 1 h in the presence or absence of various amounts of the different soR adapter proteins, which had been pretreated in the presence (+) or absence (−) of DTT. At 7 h after inoculation, luciferase expression was determined. Shown is the percentage of neutralization, calculated as the decrease in luciferase expression relative to infections in the absence of adapter proteins. The data represent the average of a representative experiment performed in triplicate. Error bars indicate standard deviations. (C) MHV-EFLM (10^4 $TCID_{50}$) was inoculated onto 10^5 A431 cells in the presence of 5 nM soR-425 or soR-h-425 protein, both pretreated in the presence (+) or in the absence (−) of 1.56 μM DTT. After 1 h, the cells were washed and incubation was continued for 20 h, after which the cells were lysed and luciferase expression measured. All data shown represent the average and standard deviation of an experiment performed in triplicate. RLU, relative light units.

or mock supernatant did not induce detectable luciferase expression (not shown). Interestingly, whereas the presence of the hinge region appeared to enhance the efficiency of virus neutralization by the adapter protein (Fig. 3), it resulted in a significant, approximately 10-fold, decrease in targeting efficiency.

Soluble receptor-mediated MHV neutralization, but not targeting, is affected by soR dimer formation. To further investigate the effect of the hinge region in the soR proteins on MHV neutralization and targeting, we disrupted the soR-h and soR-h-425 dimers by treatment with the minimal concentration of dithiothreitol (DTT) required for complete reduction of the hinge disulfide bonds. Thus, all soR proteins were treated with 1.56 μM DTT for 20 min at 4°C. Dimer dissociation was confirmed by Western blot analysis performed under nonreducing conditions (Fig. 5A). Incubation of soR-h and soR-h-425 in the presence of DTT resulted in full reduction to monomers, whereas in the absence of DTT, protein bands corresponding to the size of dimers were detected. No effects of the DTT treatment on soR and soR-425 migration were observed.

Next, we analyzed whether the reduced soR-h and soR-h-425 proteins displayed neutralization and targeting efficiencies similar to those of their counterparts lacking the hinge region. MHV-EFLM was inoculated onto murine LR7 cells in the presence of the different soR proteins, each pretreated in the presence or absence of DTT. After 7 h of incubation, the cells were lysed and luciferase expression was measured. As shown in Fig. 5B, after reduction the soR-h and soR-h-425 proteins lost their enhanced neutralization capacities relative to the soR and soR-425 proteins, which both lack the hinge dimerization region. These results indicate that dimerization of the soR proteins has a beneficial effect on MHV neutralization. We also determined the effect of reduction of the soR-h-425 dimers on MHV targeting. MHV-EFLM was inoculated onto A431 cells in the presence of 5 nM soR-425 or soR-h-425 protein, both pretreated in the presence or absence of DTT. After 1 h, the cells were washed and incubation was continued for 20 h, after which the cells were lysed and luciferase expression measured. Interestingly, whereas dimer reduction had a profound effect on the neutralization capacity of soR-h-425, no significant DTT-mediated effects on targeting efficiency were observed (Fig. 5C).

Soluble receptor-mediated coronavirus infection is EGFR and S protein specific. To further confirm that the infection of MHV-EFLM established by soR-425 or soR-h-425 was indeed mediated by the EGFR expressed on A431 cells, we studied the effect of anti-EGFR MAb 425. A431 cells were incubated

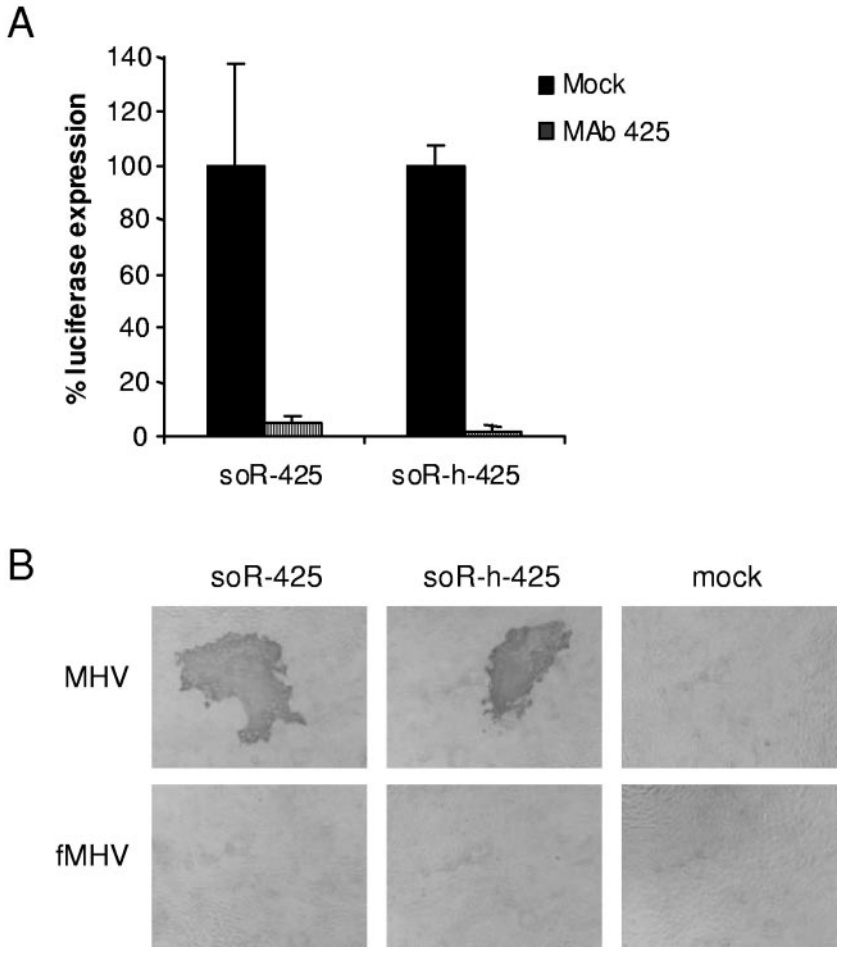

FIG. 6. EGFR- and spike-specific coronavirus targeting. (A) MHV-EFLM was preincubated with soR-425 or soR-h-425 and inoculated onto A431 cells preincubated for 1 h at 4°C in the presence or absence of anti-EGFR MAb 425. The data represent average luciferase expression relative to that of cells inoculated in the absence of blocking antibody. Error bars show the standard deviations of experiments performed in triplicate. (B) The specificity of the interaction of the soR adapters with the MHV spike was determined by preincubating 10^4 $TCID_{50}$ of MHV or fMHV in the presence or absence of the soR adapters at 0.5 nM. After 1 h, the inoculum was replaced with normal culture medium and incubation was continued for 20 h. Polyclonal MHV antibodies were used to detect the presence of coronavirus proteins in the A431 cells at 20 h after inoculation. Representative images are shown.

with the antibody prior to inoculation with MHV-EFLM in the presence of 0.5 nM soR-425 or soR-h-425 for 1 h. The cells were then washed and incubation continued for 20 h. Figure 6A shows that infection was blocked almost completely by MAb 425, confirming that a direct interaction with the EGFR is required for adapter-mediated infection.

To verify that the interaction of the soR adapters with MHV was S protein specific, MHV-EFLM or fMHV was preincubated with the soR-425 or soR-h-425 protein and inoculated onto A431 cells. The chimeric virus fMHV carries S proteins the ectodomain of which is derived from FIPV. It infects cells through the feline aminopeptidase N molecule rather than murine CEACAM1a (21). Immunostaining for coronavirus proteins was performed at 20 h after inoculation to determine whether the A431 cells had been infected. Only the cells inoculated with MHV-EFLM stained positive, whereas cells inoculated with fMHV remained negative (Fig. 6B). These results demonstrated that the MHV spike ectodomain is essential for CEACAM1a N domain-mediated infection. In addition, the immunostaining revealed the presence of large spots of fused cells, typical for MHV infections of murine cells. The results collectively indicate that the targeted infections of MHV in the presence of soR-425 or soR-h-425 are dependent on interactions of the adapter proteins both with the MHV spike and with the human EGFR.

Targeted coronavirus infections require S protein-mediated membrane fusion. Addition of a heptad repeat-mimicking peptide, mHR2, during inoculation of murine LR7 cells abrogates MHV infection by inhibition of the coalescence of the heptad repeat regions, HR1 and HR2, required for fusion (2). In order to investigate whether the targeted MHV infections also depend on those conformational rearrangements in the viral spike protein, we tested their sensitivity to the mHR2 peptide. To this end, MHV-EFLM was targeted toward EGFR expressed on A431 cells with 5 nM adapter proteins soR-425 and soR-h-425, in the presence or absence of 20 μM mHR2. As shown in Fig. 7, addition of the peptide efficiently blocked both soR-425- and soR-h-425-mediated infections. Thus, EGFR-

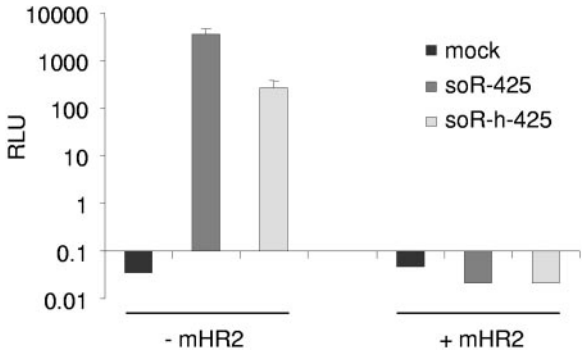

FIG. 7. Effect of mHR2 on the bispecific adapter-mediated entry process. A431 cells were inoculated with a preincubated mixture of MHV-EFLM (10^4 $TCID_{50}$) and 5 nM soR-425 or soR-h-425 in the presence or absence of 20 μM mHR2. After 1 h, the cells were washed and incubation continued for 20 h. Finally, the cells were lysed and luciferase activity was measured. Error bars show the standard deviations of experiments performed in triplicate. RLU, relative light units.

mediated MHV infections appear to depend on conformational changes in the S protein, similar to the ones occurring during normal infection.

Soluble receptor-mediated syncytium formation and production of progeny virus. Interestingly, A431 cells infected by EGFR-targeted MHV showed cell-cell fusion typical for coronaviruses (Fig. 6B). To investigate whether syncytium formation between infected and neighboring cells resulted from undefined interactions or from specific bridging by the adapter protein, A431 cells were inoculated with MHV-EFLM in 5 nM soR-425-containing medium for 2 h. The cells were washed and subsequently cultured for another 22 h in the presence or absence of 5 nM soR-425 or soR. Thus, soR-425 was either present continuously to mediate both infection and syncytium formation or only briefly to mediate the targeted infection. Removal of soR-425 after 2 h did not have a significant effect on the number of syncytia observed for each inoculated cell culture (data not shown); however, we did observe a reduction of the extent of syncytium formation by approximately threefold (Fig. 8A). The addition of soR proteins, which lack the scFv 425 domain, did not result in increased cell-cell fusion, indicating an EGFR-related effect. Hence, soR-425 may promote fusion not only between the MHV envelope and target cells during virus entry but also between MHV-infected and neighboring cells in the course of the infection process.

Finally, we determined whether the soR-425-mediated infection was productive and yielded infectious virus. A431 cells were inoculated with MHV-EFLM (MOI, 5) that had been preincubated in the presence or absence of 5 nM soR-425 or soR-h-425 and were then incubated for 1 h. They were then washed and incubated further, and samples were taken from the culture medium at different time points after inoculation for titration on murine LR7 cells. As depicted in Fig. 8B, virus preincubated in the presence of soR-425 or soR-h-425 produced progeny virus reaching titers of up to 10^5 to 10^6 $TCID_{50}$/ml. In contrast, inoculation with MHV-EFLM in the absence of adapter protein did not lead to detectable virus production. Thus, adapter-mediated redirection of MHV to human cells results in the formation and secretion of progeny virus.

DISCUSSION

Recently, the use of viruses as potential tools to complement the conventional treatment options for cancer therapy has gained considerable interest (28, 30). In this study, we demonstrate that the mouse coronavirus MHV may be an attractive candidate for this purpose. MHV has a narrow species tropism and a strong capacity to kill cells. These features might be used to advantage by controlled targeting of the virus to human tumor cells. Using the specificity of the mCEACAM1a MHV

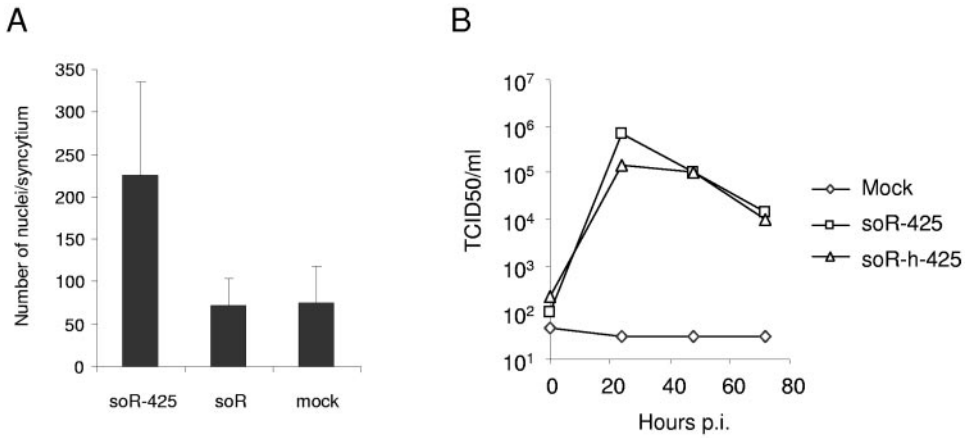

FIG. 8. Soluble receptor-mediated syncytium formation and production of progeny virus after targeted infection. (A) A431 cells were inoculated with MHV-EFLM in soR-425-containing medium for 2 h and subsequently cultured for another 22 h in the presence or absence of soR-425 or soR. The cells were fixed and stained for the presence of coronavirus proteins with polyclonal MHV antibodies. The number of nuclei of eight randomly selected syncytia per inoculated, stained cell culture was determined under a light microscope, and this was carried out in parallel in triplicate. The data represent the average number of nuclei per syncytium, based in each case on the counting of 24 syncytia. Error bars show the standard deviation of such an experiment. (B) MHV-EFLM was preincubated in the presence or absence of soR-425 or soR-h-425 and inoculated onto A431 cells. After 1 h, the cells were washed and incubation was continued. At several time points thereafter, samples were taken from the cell culture medium and subsequently titrated on murine LR7 cells to determine the amount of virus produced. The results shown are from a representative experiment. p.i., postinoculation.

receptor, we constructed bispecific adapter molecules composed of the S protein-binding fragment of this receptor coupled to an antibody fragment directed to the human EGFR, which is known to be overexpressed on cells of many human cancers. The adapter proteins were found to effectively mediate infection of EGFR-expressing human A431 cancer cells. Cell entry appeared to be effected through the normal spike protein-driven membrane fusion mechanism, and the infection resulted in efficient formation of syncytia, which we observed earlier to ultimately lead to efficient eradication of the culture (39).

We have shown recently that targeted entry of the feline coronavirus FIPV and chimeric fMHV could also be accomplished by making use of an adapter composed of two single-chain antibodies, one directed against the feline viral spike and the other to the EGFR (39). Like the soR-425-mediated MHV infections, the bispecific antibody-mediated fMHV infections were blocked by an HR-mimicking peptide derived in this case from the feline S protein (39). These observations suggest that binding of the adapters to particular regions of the S protein—i.e., the receptor-binding domain or a certain epitope—results in conformational changes that, upon binding of the virus-adapter complex to a cellular target receptor, facilitate insertion of the fusion peptide into the cell membrane. Binding of these adapters apparently does not inactivate the virus, as is also indicated by studies in which MHV, purified by sedimentation through a sucrose cushion after preincubation of the virus with the soR-425 adapter protein, maintained its infectivity for EGFR-positive cells (our unpublished data). These results suggest that the adapter proteins, once bound to the virus, may freeze the S protein in a stable prefusion conformation ready to proceed to its structural rearrangements upon contacting the target cell. What the actual trigger is that activates the fusion process is unknown, but it is quite likely that the insertion of the fusion peptide into the cellular membrane is a critical event.

An interesting paradox that we noticed in our studies was the opposite efficiency of hinge-containing and hingeless adapter molecules in neutralization and targeting. Thus, the virus-neutralizing capacities of the adapters soR-h and soR-h-425 were significantly higher than those of the soR and soR-425 molecules, respectively, while the reverse was true of the relative targeting efficiencies of soR-h-425 and soR-425 (Fig. 3 to 5). The reasons for these differences appear to be unrelated. This can be concluded from the differential effects of reducing agent treatment of the adapters on the two activities. Whereas this treatment did not affect the targeting efficiencies of the adapters, it reduced the virus-neutralizing capacities of the hinge-containing adapters to about the level of their hingeless counterparts, the activity of which was not significantly changed by the treatment. Dimeric forms of the adapters apparently neutralize the infectivity of the virus more efficiently than monomers, possibly by their stronger interaction with the spikes or their ability to cross-link spikes on the viral particle. Remarkable as it may seem, these effects apparently have no bearing on the efficiency of the targeting of such viral particles or on the subsequent steps leading to membrane fusion.

Previous studies have shown that the N domain of the mCEACAM1a receptor is sufficient by itself to induce conformational changes in the MHV spike protein (22, 24, 34, 40). Remarkably, however, this same N domain, when linked directly to the transmembrane domain, thus lacking the intermediate CEACAM1a A2 domain (Fig. 1), failed to function as a receptor for MHV (9). A possible explanation for this observation might be that the functional structure of the N domain is affected by linking it to the transmembrane region. This appeared, however, not to be the case when the N domain was replacing the corresponding domain in the mouse poliovirus receptor homolog (25), which also belongs to the family of Ig-like viral receptors (23). The resulting chimeric receptor molecule functioned as a receptor for MHV (6). It is conceivable that the CEACAM1a N domain needs a certain distance from the cellular membrane to allow interaction with the S protein to lead to effective membrane fusion. Interestingly, the efficiency of the targeted infections described here was significantly higher with the soR-425 adapter than with the soR-h-425 adapter, and this difference was not accounted for by the dimeric state of a fraction of the latter, as the targeting efficiency of the hinge-containing adapter was unaffected by dissociation through DTT treatment. These observations indeed suggest that also the dimensions of our adapters may affect the efficiency of their targeting. Whether this is really the case, and how, remains to be investigated.

The ability to target viruses by design to preselected cells is a tremendous challenge with far-reaching implications for the development of virus-based therapies. We previously established the principle of retargeting of coronaviruses by exchanging spike ectodomains (16, 21). Subsequent attempts to modify the tropism of these viruses further by incorporating tumor-binding ligands into different parts of the spike protein were unsuccessful, as no viable viruses could be rescued (M. H. Verheije, T. Würdinger, and P. J. M. Rottier, unpublished data). As an alternative and potentially also versatile targeting approach, we therefore aimed at the development of bispecific adapters. The use of soluble receptor-based adapters to expand virus tropism has been described before for retroviruses (32) and adenoviruses (20). Recently, also the herpes simplex virus was redirected to a new receptor via the variable domain of its cellular receptor, nectin 1, fused to a single-chain antibody (27). However, in contrast to these viruses, the coronavirus MHV is normally incapable of infecting human cells, due to its restricted tropism. Hence, its native tropism does not need to be eliminated to obtain a truly targeted virus, which avoids possible reduction of its cytotoxicity to the specific target cells. In order to fully exploit the oncolytic properties of MHV, multiround genetic targeting will be essential. As we described earlier, incorporation of the gene encoding the bispecific single-chain antibody s11-425 into the adenovirus genome leads to persistent self-targeting of the virus to a specific receptor (35). Also others showed virus retargeting by genomically expressed bispecific adapters, though this resulted in a reduction of the oncolytic potency of the adenovirus in the case of the sCAR-EGF adapter (19). The same approach seems also feasible for the development of tumor-targeted coronaviruses. As we and others showed recently, MHV can tolerate and express foreign genes from various insertion sites of its genome (4, 5, 11, 12). Therefore, our next step in the development of oncolytic coronaviruses will be to introduce the gene encoding a bispecific adapter molecule into the virus genome.

ACKNOWLEDGMENTS

We are grateful to T. Gallagher for providing the N-CEACAM-Fc expression construct and the anti-N-CEACAM-Fc polyclonal antibodies.

This work was supported by the Dutch Cancer Society (UU 2001-2430). Victor W. van Beusechem is supported by a research fellowship from the Royal Netherlands Academy of Arts and Sciences (KNAW).

REFERENCES

1. **Beauchemin, N., T. Chen, P. Draber, G. S. Dveksler, P. Gold, S. Gray-Owen, F. Grunert, S. Hammarstrom, K. V. Holmes, A. Karlsson, M. Kuroki, S. H. Lin, L. Lucka, S. M. Najjar, M. Neumaier, B. Obrink, J. E. Shively, K. M. Skubitz, C. P. Stanners, P. Thomas, J. A. Thompson, M. Virji, S. von Kleist, C. Wagener, S. Watt, and W. Zimmermann.** 1999. Redefined nomenclature for members of the carcinoembryonic antigen family. Exp. Cell Res. **252:** 243–249.
2. **Bosch, B. J., R. van der Zee, C. A. de Haan, and P. J. Rottier.** 2003. The coronavirus spike protein is a class I virus fusion protein: structural and functional characterization of the fusion core complex. J. Virol. **77:**8801–8811.
3. **Compton, S. R., C. B. Stephensen, S. W. Snyder, D. G. Weismiller, and K. V. Holmes.** 1992. Coronavirus species specificity: murine coronavirus binds to a mouse-specific epitope on its carcinoembryonic antigen-related receptor glycoprotein. J. Virol. **66:**7420–7428.
4. **de Haan, C. A. M., B. J. Haijema, D. Boss, F. W. H. Heuts, and P. J. M. Rottier.** 2005. Coronaviruses as vectors: stability of foreign gene expression. J. Virol. **79:**12742–12751.
5. **de Haan, C. A., L. van Genne, J. N. Stoop, H. Volders, and P. J. Rottier.** 2003. Coronaviruses as vectors: position dependence of foreign gene expression. J. Virol. **77:**11312–11323.
6. **Dveksler, G. S., A. A. Basile, C. B. Cardellichio, and K. V. Holmes.** 1995. Mouse hepatitis virus receptor activities of an MHVR/mph chimera and MHVR mutants lacking N-linked glycosylation of the N-terminal domain. J. Virol. **69:**543–546.
7. **Dveksler, G. S., C. W. Dieffenbach, C. B. Cardellichio, K. McCuaig, M. N. Pensiero, G. S. Jiang, N. Beauchemin, and K. V. Holmes.** 1993. Several members of the mouse carcinoembryonic antigen-related glycoprotein family are functional receptors for the coronavirus mouse hepatitis virus A59. J. Virol. **67:**1–8.
8. **Dveksler, G. S., M. N. Pensiero, C. B. Cardellichio, R. K. Williams, G. S. Jiang, K. V. Holmes, and C. W. Dieffenbach.** 1991. Cloning of the mouse hepatitis virus (MHV) receptor: expression in human and hamster cell lines confers susceptibility to MHV. J. Virol. **65:**6881–6891.
9. **Dveksler, G. S., M. N. Pensiero, C. W. Dieffenbach, C. B. Cardellichio, A. A. Basile, P. E. Elia, and K. V. Holmes.** 1993. Mouse hepatitis virus strain A59 and blocking antireceptor monoclonal antibody bind to the N-terminal domain of cellular receptor. Proc. Natl. Acad. Sci. USA **90:**1716–1720.
10. **Elroy-Stein, O., and B. Moss.** 1990. Cytoplasmic expression system based on constitutive synthesis of bacteriophage T7 RNA polymerase in mammalian cells. Proc. Natl. Acad. Sci. USA **87:**6743–6747.
11. **Enjuanes, L., I. Sola, F. Almazan, J. Ortego, A. Izeta, J. M. Gonzalez, S. Alonso, J. M. Sanchez, D. Escors, E. Calvo, C. Riquelme, and C. Sanchez.** 2001. Coronavirus derived expression systems. J. Biotechnol. **88:**183–204.
12. **Fischer, F., C. F. Stegen, C. A. Koetzner, and P. S. Masters.** 1997. Analysis of a recombinant mouse hepatitis virus expressing a foreign gene reveals a novel aspect of coronavirus transcription. J. Virol. **71:**5148–5160.
13. **Frana, M. F., J. N. Behnke, L. S. Sturman, and K. V. Holmes.** 1985. Proteolytic cleavage of the E2 glycoprotein of murine coronavirus: host-dependent differences in proteolytic cleavage and cell fusion. J. Virol. **56:**912–920.
14. **Galanis, E., R. Vile, and S. J. Russell.** 2001. Delivery systems intended for in vivo gene therapy of cancer: targeting and replication competent viral vectors. Crit. Rev. Oncol. Hematol. **38:**177–192.
15. **Gallagher, T. M.** 1997. A role for naturally occurring variation of the murine coronavirus spike protein in stabilizing association with the cellular receptor. J. Virol. **71:**3129–3137.
16. **Haijema, B. J., H. Volders, and P. J. Rottier.** 2003. Switching species tropism: an effective way to manipulate the feline coronavirus genome. J. Virol. **77:**4528–4538.
17. **Haisma, H. J., J. Grill, D. T. Curiel, S. Hoogeland, V. W. van Beusechem, H. M. Pinedo, and W. R. Gerritsen.** 2000. Targeting of adenoviral vectors through a bispecific single-chain antibody. Cancer Gene Ther. **7:**901–904.
18. **Hemmila, E., C. Turbide, M. Olson, S. Jothy, K. V. Holmes, and N. Beauchemin.** 2004. *Ceacam1a*$^{-/-}$ mice are completely resistant to infection by murine coronavirus mouse hepatitis virus A59. J. Virol. **78:**10156–10165.
19. **Hemminki, A., M. Wang, T. Hakkarainen, R. A. Desmond, J. Wahlfors, and D. T. Curiel.** 2003. Production of an EGFR targeting molecule from a conditionally replicating adenovirus impairs its oncolytic potential. Cancer Gene Ther. **10:**583–588.
20. **Kashentseva, E. A., T. Seki, D. T. Curiel, and I. P. Dmitriev.** 2002. Adenovirus targeting to c-erbB-2 oncoprotein by single-chain antibody fused to trimeric form of adenovirus receptor ectodomain. Cancer Res. **62:**609–616.
21. **Kuo, L., G. J. Godeke, M. J. Raamsman, P. S. Masters, and P. J. Rottier.** 2000. Retargeting of coronavirus by substitution of the spike glycoprotein ectodomain: crossing the host cell species barrier. J. Virol. **74:**1393–1406.
22. **Matsuyama, S., and F. Taguchi.** 2002. Receptor-induced conformational changes of murine coronavirus spike protein. J. Virol. **76:**11819–11826.
23. **Mendelsohn, C. L., E. Wimmer, and V. R. Racaniello.** 1989. Cellular receptor for poliovirus: molecular cloning, nucleotide sequence, and expression of a new member of the immunoglobulin superfamily. Cell **56:**855–865.
24. **Miura, H. S., K. Nakagaki, and F. Taguchi.** 2004. N-terminal domain of the murine coronavirus receptor CEACAM1 is responsible for fusogenic activation and conformational changes of the spike protein. J. Virol. **78:**216–223.
25. **Morrison, M. E., and V. R. Racaniello.** 1992. Molecular cloning and expression of a murine homolog of the human poliovirus receptor gene. J. Virol. **66:**2807–2813.
26. **Muller, K. M., K. M. Arndt, and A. Pluckthun.** 1998. A dimeric bispecific miniantibody combines two specificities with avidity. FEBS Lett. **432:**45–49.
27. **Nakano, K., R. Asano, K. Tsumoto, H. Kwon, W. F. Goins, I. Kumagai, J. B. Cohen, and J. C. Glorioso.** 2005. Herpes simplex virus targeting to the EGF receptor by a gD-specific soluble bridging molecule. Mol. Ther. **11:**617–626.
28. **Ring, C. J.** 2002. Cytolytic viruses as potential anti-cancer agents. J. Gen. Virol. **83:**491–502.
29. **Rottier, P. J., M. C. Horzinek, and B. A. van der Zeijst.** 1981. Viral protein synthesis in mouse hepatitis virus strain A59-infected cells: effect of tunicamycin. J. Virol. **40:**350–357.
30. **Russell, S. J.** 2002. RNA viruses as virotherapy agents. Cancer Gene Ther. **9:**961–966.
31. **Sainz, B. J., J. M. Rausch, W. R. Gallaherm, R. F. Garrym, and W. C. Wimley.** 2005. The aromatic domain of the coronavirus class I viral fusion protein induces membrane permeabilization: putative role during viral entry. Biochemistry **44:**947–958.
32. **Snitkovsky, S., and J. A. Young.** 1998. Cell-specific viral targeting mediated by a soluble retroviral receptor-ligand fusion protein. Proc. Natl. Acad. Sci. USA **95:**7063–7068.
33. **Tan, K., B. D. Zelus, R. Meijers, J. H. Liu, J. M. Bergelson, N. Duke, R. Zhang, A. Joachimiak, K. V. Holmes, and J. H. Wang.** 2002. Crystal structure of murine sCEACAM1a[1,4]: a coronavirus receptor in the CEA family. EMBO J. **21:**2076–2086.
34. **Tsai, J. C., B. D. Zelus, K. V. Holmes, and S. R. Weiss.** 2003. The N-terminal domain of the murine coronavirus spike glycoprotein determines the CEACAM1 receptor specificity of the virus strain. J. Virol. **77:**841–850.
35. **van Beusechem, V. W., D. C. Mastenbroek, P. B. van den Doel, M. L. Lamfers, J. Grill, T. Wurdinger, H. J. Haisma, H. M. Pinedo, and W. R. Gerritsen.** 2003. Conditionally replicative adenovirus expressing a targeting adapter molecule exhibits enhanced oncolytic potency on CAR-deficient tumors. Gene Ther. **10:**1982–1991.
36. **Wessner, D. R., P. C. Shick, J. H. Lu, C. B. Cardellichio, S. E. Gagneten, N. Beauchemin, K. V. Holmes, and G. S. Dveksler.** 1998. Mutational analysis of the virus and monoclonal antibody binding sites in MHVR, the cellular receptor of the murine coronavirus mouse hepatitis virus strain A59. J. Virol. **72:**1941–1948.
37. **Wickham, T. J.** 2003. Ligand-directed targeting of genes to the site of disease. Nat. Med. **9:**135–139.
38. **Williams, R. K., G. S. Jiang, and K. V. Holmes.** 1991. Receptor for mouse hepatitis virus is a member of the carcinoembryonic antigen family of glycoproteins. Proc. Natl. Acad. Sci. USA **88:**5533–5536.
39. **Würdinger, T., M. H. Verheije, M. Raaben, B. J. Bosch, C. A. de Haan, V. W. van Beusechem, P. J. Rottier, and W. R. Gerritsen.** 2005. Targeting non-human coronaviruses to human cancer cells using a bispecific single-chain antibody. Gene Ther. **12:**1394–1404.
40. **Zelus, B. D., J. H. Schickli, D. M. Blau, S. R. Weiss, and K. V. Holmes.** 2003. Conformational changes in the spike glycoprotein of murine coronavirus are induced at 37°C either by soluble murine CEACAM1 receptors or by pH 8. J. Virol. **77:**830–840.